INL/CON-14-31079
PREPRINT

THE COUPLING OF THE NEUTRON TRANSPORT APPLICATION RATTLESNAKE TO THE NUCLEAR FUELS PERFORMANCE APPLICATION BISON UNDER THE MOOSE FRAMEWORK

PHYSOR 2014

Frederick N. Gleicher, Javier Ortensi, Benjamin W. Spencer, Yaqi Wang, Stephen R. Novascone, Jason D. Hales, Derek Gaston, Richard L. Williamson, Richard C. Martineau

October 2014

The INL is a
U.S. Department of Energy
National Laboratory
operated by
Battelle Energy Alliance

This is a preprint of a paper intended for publication in a journal or proceedings. Since changes may be made before publication, this preprint should not be cited or reproduced without permission of the author. This document was prepared as an account of work sponsored by an agency of the United States Government. Neither the United States Government nor any agency thereof, or any of their employees, makes any warranty, expressed or implied, or assumes any legal liability or responsibility for any third party's use, or the results of such use, of any information, apparatus, product or process disclosed in this report, or represents that its use by such third party would not infringe privately owned rights. The views expressed in this paper are not necessarily those of the United States Government or the sponsoring agency.

PHYSOR 2014 - The Role of Reactor Physics toward a Sustainable Future
The Westin Miyako, Kyoto, Japan, September 28 - October 3, 2014, on CD-ROM (2014)

THE COUPLING OF THE NEUTRON TRANSPORT APPLICATION RATTLES*N*AKE TO THE NUCLEAR FUELS PERFORMANCE APPLICATION BISON UNDER THE MOOSE FRAMEWORK

Frederick N. Gleicher*, Javier Ortensi, Benjamin W. Spencer, Yaqi Wang, Stephen R. Novascone, Jason D. Hales, Derek Gaston, Richard L. Williamson, Richard C. Martineau
Idaho National Laboratory & 2525 N. Freemont Avenue
P.O. Box 1625, Idaho Falls, Idaho, USA
Frederick.Gleicher@inl.gov, Javier.Ortensi@inl.gov, Benjamin.Spencer@inl.gov,
Yaqi.Wang@inl.gov, Stephen.Novascone@inl.gov, Jason.Hales@inl.gov,
Derek.Gaston@inl.gov,
Richard.Williamson@inl.gov, Richard.Martineau@inl.gov

ABSTRACT

The MOOSE based reactor physics tool MAMMOTH provides the capability to seamlessly couple the neutron transport application RATTLES*N*AKE to the fuels performance application BISON to produce a higher fidelity tool for fuel performance simulations. The ultimate purpose of this coupling is to provide a tool with the predictive capabilities to gain new knowledge and help resolve fundamental questions in the fuel performance arena, i.e. high-burnup structures, pellet-cladding interaction, missing pellet surface, etc. RATTLES*N*AKE solves the self-adjoint angular flux transport equation, derived from the linearized Boltzmann transport equation, and provides a sub-pin level resolution of the multigroup neutron flux. BISON solves the coupled thermomechanical equations for the fuel on a sub-millimeter scale. The coupling within the MOOSE framework allows both applications to solve their respective systems on aligned and unaligned unstructured finite element meshes. MAMMOTH uses the power density calculated by RATTLES*N*AKE to compute the local burnup evolution. Subsequently, MAMMOTH transfers the power density and burnup distribution to BISON with the MOOSE Multiapp transfer system. BISON in turn is able to provide sub-pin level temperature for cross section feed back effects. Multiple depletion cases were run with one-way and two-way data transfer in MAMMOTH for RATTLES*N*AKE-BISON. The one-way eigenvalues obtained show good agreement with the reference values obtained from the lattice physics code DRAGON4 while the two-way eigenvalue show expected differences. The power distributions obtained are consistent with both DRAGON4 and the SERPENT Monte Carlo code. The one-way and two-way calculations produce power density results that are comparable with those of the internal, static, Lassmann-style model in BISON. Differences in the power densities arise from the use of better neutron energy deposition parameters obtained from the DRAGON4 tabulations, and differences in the fuel temperature arise from a different thermal expansion models in the fuel.

Key Words: **MAMMOTH, RATTLES*N*AKE, neutron transport, fuels performance, BISON, high burn up structures, multiphysics**

*Corresponding author

1. INTRODUCTION

Fuel performance codes are often used to analyze low enriched Light Water Reactor (LWR) fuel as it is burned in the reactor. For low enriched fuels, the ^{238}U is converted to ^{239}Pu by neutron capture; this occurs because ^{238}U has a strong absorption resonance at 6.68 eV. The ^{239}Pu is also converted into heavier plutonium isotopes with the absorption of more neutrons. The plutonium isotopes act as extra fissile material on the outer edge of the fuel pin, resulting in an increase in the fission rate density relative to the inner region of the fuel pin, and contribute significantly to the fuel rod power at higher burnup [1]. The increase in the fission rate density is often called the neutronic rim effect [2, 3]. The neutronic rim effect is significant not only due to the extra fission occurring on the surface of the fuel pin, but also due to the self-shielding by the plutonium, which depresses the fission rate density in the inner region of the fuel pin. To account for this effect, fuel performance codes usually have an empirical radial power distribution derived with parameters obtained numerically from transport codes such as HELIOS or MCNP [2, 4, 5] or have parameters fitted from reactor experiments [6]. The current internal models in the fuel performance codes have a number of limitations. The models assume that the power density distribution is separable into azimuthal, axial, and radial components where the radial distribution is supplied by the methods mentioned above. These models are derived from conditions in which the neutron flux is slowly varying in space and energy such as the quasi-steady state conditions used in depletion calculations [2, 3]. Finally, these models do not account for temperature feedback, coolant density feedback, or other reactor elements such as water holes or different fuel elements which affect the neutron flux distribution [7–9].

An attempt to address these limitations has been investigated in prior work, where the radiation transport applications are coupled to fuel performance applications [10–13]. The PLUTON depletion code [10] was coupled to the fuels performance code FEMAXI [14] and assumes three energy groups for the scalar flux. A point source transport model in the radial direction is used to calculate the epithermal flux distribution for the resonance structure, but similar to the internal models of fuels performance codes, a diffusion based analytic solution is used for the radial power distribution. Also similar to the internal models of fuels performance codes, this flux distribution is applied only in the radial direction; unlike the internal models, the microscopic cross sections are temperature dependent. Despite the temperature dependent cross section physics PLUTON still has some of the limitations outlined for the internal fuel performance models.

Moreover, the Deterministic Core Analysis based on Ray Tracing (DeCART) application [15] was coupled to the finite element fuels performance application BISON [16] to create a combined application [12]. For this coupling the power density rate was mapped from finite volume type mesh in DeCART to finite element mesh in BISON with a point mapping scheme that does not preserve the total power of the fuel pin. A correction to the power density must be made to preserve the total power of the fuel pin and in some cases could result in a significant alteration of the mapped power density [12]. The temperature profile calculated in BISON was mapped back to DeCART by computing the average temperature for each DeCART finite volume region on the BISON finite element mesh. For this coupling the temperature feedback was observed to change the pin eigenvalue when compared to a similar calculation with an assigned fuel temperature and require only one Picard iteration. This coupling overcomes a number of the limitations for the internal fuel performance models, but poor choices in the meshing can cause problems in getting higher fidelity solutions.

Also DeCART is made specifically for LWR analysis and can only treat pin cell geometries.

Furthermore, the core analysis applications DeCART and the Purdue Advanced Reactor Core Simulator (PARCS) [17] were coupled to the finite element fuels performance code FALCON [18] to examine a reactivity insertion in the core [11]. For these couplings the DeCART/PARCS power density was mapped either onto a axisymmetric (r,z) or radial plane (r,θ) FALCON finite element mesh. The fidelity of the different mappings of the power distribution were not discussed. Calculations were performed to obtain the strain energy density during the reactivity insertion. Differences were found between the DeCART pin resolved calculations and the PARCS nodal homogenized calculations, and neither calculation resulted in a strain energy density above the critical strain energy density. For this coupling, limitations include the 2-D nature of FALCON since only (r,z) or (r,θ) calculations can be performed. Other problems include the fidelity of temperature feedback since the neutronics temperature distribution and the fuel performance temperature distribution appear to be separate.

In addition, the transport code Denovo was coupled to the Advanced Multi-Physics Nuclear Fuel Performance program (AMPFuel) [13]. Denovo solves the steady state neutron transport equation with the discrete ordinates (S_N) method on a Cartesian mesh [19] and AMP solves the thermomechanical equations on unstructured mesh. The coupling between codes was achieved by mapping the power density from Denovo to AMPFuel. The power density, calculated on a structured mesh by Denovo, was reconstructed in AMPFuel with Zernike polynomials [20]. A limitation of this coupling is the structured Cartesian mesh must be very fine to resolve the cylindrical pin geometry for practical LWR applications, and this method of coupling has been achieved only with fresh fuel under steady state conditions.

Given the limitations discussed above for this important problem, alternate neutronic and fuel performance simulation software was chosen for coupling. RATTLES*N*AKE is a 3D finite element based neutron transport application developed using the Multiphysics Object Oriented Simulation Environment (MOOSE) [21], and solves the Self-Adjoint Angular Flux (SAAF) formulation of the neutron transport equation using the Jacobian-Free Newton Krylov (JFNK) method [22]. Because RATTLES*N*AKE is under the MOOSE framework, RATTLES*N*AKE can solve the SAAF transport equation on a given structured or unstructured finite element mesh. This flexibility allows RATTLES*N*AKE to solve the SAAF transport equation on light water reactor pin resolved grids and other reactor geometries as well.

BISON is a 3D finite element based fuel performance code also developed on the MOOSE framework [16]. BISON implicitly solves coupled thermomechanical equations over the domain of a single fuel rod using the JFNK method [22]. BISON includes models for: thermal and irradiation creep in the fuel and cladding, swelling and densification, gap heat transfer, and the gap and plenum pressure. BISON also can model the thermal and mechanical contact between the fuel and cladding. The coupling of RATTLES*N*AKE and BISON provides a multiphysics tool for fuel performance analysis that is more consistent with first principle physics and that has higher spatial resolution than any other code system currently available. This new multiphysics capability is developed under a new MOOSE-based reactor physics application named MAMMOTH. MAMMOTH is able to provide to BISON a spatially detailed description of the power density, fast neutron flux, and burnup distribution throughout the fuel lifetime based on the RATTLES*N*AKE flux solution. BISON provides MAMMOTH with a detailed and accurate pin level temperature field for feedback effects

on the neutron flux distribution.

2. GOVERNING EQUATIONS OVERVIEW

In the two sections below, the governing equations for fuel performance and neutronics are briefly overviewed and discussed. Due to length, only the mono-energetic form of the second order transport equation with isotropic scattering is given. The description of the full equation with the methods applied in solving the equation can be found in the literature [21, 23–27].

2.1. OVERVIEW OF THE GOVERNING EQUATIONS IN RATTLES*N*AKE

The self-adjoint angular flux (SAAF) formulation of the linear Boltzmann transport equation with the continuous finite element method (CFEM) for the spatial discretization, with the discrete ordinates method (S_N) for the angular discretization, has been studied in the past [23–26]. It has the angular flux as the direct unknowns in contrast to the even-odd parity formulations. This discretization scheme, referred to as SAAF-SN-CFEM in this paper, is classified as a second-order transport scheme [23] because of the order of its streaming operator with respect to the spatial variable. Compared with other transport discretization schemes, it offers some advantages which are quite appealing for multiphysics simulations where massively parallel computing over the heterogeneous domain is generally desired [27]. The SAAF form of the transport equation used in RATTLES*N*AKE can be derived from the first order Boltzmann form of the transport equation [23]. The monoenergetic self-adjoint angular flux transport equation with position $\vec{r}$ in the solution domain $\mathcal{D}$ and streaming direction $\vec{\Omega}$ on the two-dimensional unit sphere $\mathcal{S}$ is

$$-\vec{\nabla}\cdot\frac{\vec{\Omega}\vec{\Omega}}{\sigma_t}\vec{\nabla}\Psi+\sigma_t\Psi=\frac{\sigma_{s,0}}{4\pi}\Phi+\frac{S}{4\pi}-\vec{\Omega}\cdot\vec{\nabla}\left(\frac{1}{\sigma_t}\frac{\sigma_{s,0}}{4\pi}\Phi+\frac{1}{\sigma_t}\frac{S}{4\pi}\right). \tag{1}$$

where σ_t is the total cross section and $\sigma_{s,0}$ is the isotropic scattering cross section. The source S includes the higher scattering moments as well as the fission source. The dependent variable Ψ is the angular flux and the scalar flux Φ is the integral of angular flux over the sphere $\mathcal{S}$,

$$\Phi(\vec{r})\equiv\int_{4\pi}\Psi(\vec{r},\vec{\Omega})d\Omega, \tag{2}$$

where $d\Omega=d\mu d\varpi$; μ is the cosine of the polar angle and ϖ is the azimuthal angle. The surface-source and the reflective boundary conditions for the transport equation are as follows:

$$\Psi(\vec{r}_b,\vec{\Omega})=\begin{cases}\Psi^{inc}(\vec{r}_b,\vec{\Omega}), & \vec{r}_b\in\partial\mathcal{D}^s\\ \Psi(\vec{r}_b,\vec{\Omega}_r), & \vec{r}_b\in\partial\mathcal{D}^r\end{cases} \tag{3}$$
$$\text{for } \vec{\Omega}\cdot\vec{n}_b<0,$$

where $\partial\mathcal{D}$ indicates the boundaries of the solution domain $\mathcal{D}$ and $\vec{n}_b$ is the outward unit vector at a point $\vec{r}_b$ on the boundary. The superscript s and r indicate the surface source boundary and the reflective boundary respectively. The reflective angle is

$$\vec{\Omega}_r=\vec{\Omega}-2(\vec{\Omega}\cdot\vec{n}_b)\vec{n}_b. \tag{4}$$

When the in-coming angular flux Ψ^{inc} is equal to zero, the surface-source boundary condition is known as the vacuum boundary condition. These notations are standard and are found in most textbooks, such as Ref. [28]. An additional condition on the down-wind boundaries is needed to make the solution of the continuous SAAF Eq. 1 unique. This condition is typically to let the solution satisfy the original first-order transport equation.

A macro depletion scheme was implemented to track the change in the local cross sections as the fuel is burned. The cross sections in the SAAF equation are functions of space, energy, temperature, and burnup. The cross sections are pretabulated for different temperature and burnup values and are interpolated at the local temperature and burnup. The cross section values are precalculated from codes such as SERPENT or DRAGON4 [29, 30].

2.2. OVERVIEW OF THE GOVERNING EQUATIONS IN BISON

The BISON governing equations consist of fully-coupled partial differential equations for energy, species, and momentum conservation. The energy balance is given in terms of the heat conduction equation

$$\rho C_p \frac{\partial T}{\partial t} + \nabla \cdot \mathbf{q} - E_f \dot{F} = 0, \tag{5}$$

where T, ρ and C_p are the temperature, density and specific heat, respectively, E_f is the energy released in a single fission event, and $\dot{F}$ is the volumetric fission rate. The heat flux is given as

$$\mathbf{q} = -k\nabla T, \tag{6}$$

where k denotes the thermal conductivity of the material. $\dot{F}$ can be prescribed as a function of time and space, input from a separate neutronics calculation (such as RATTLES*N*AKE), or computed based on input rod average power and axial profile data. The internal fission source model in BISON can be specified by the different functions in the MOOSE library or by separate radial, axial, azimuthal, and temporal functions [16]. The product of these functions specifies the fission rate density over the BISON mesh. The axial and temporal variation in fission rate density can be obtained from a set of linearly interpolated data, and the radial variation of the fission rate density can be determined from the internal Lassmann model [6]. Momentum conservation is prescribed assuming static equilibrium at each time increment using Cauchy's equation,

$$\nabla \cdot \sigma + \rho \mathbf{f} = 0, \tag{7}$$

where σ is the Cauchy stress tensor and $\mathbf{f}$ is the body force per unit mass (e.g. gravity). The displacement vector $\mathbf{u}$, which is the primary solution variable, is connected to the stress field via the strain, through kinematic and constitutive relations. The constitutive relationships for the fuel and clad can be functions of neutron fast flux, temperature, and burnup [16].

3. PROBLEM DEFINITION

The modelling of the inter-pin radial profile due to the ^{X}Pu buildup during the burning of the fuel rod is a challenging problem for both fuels performance and neutronics calculations. A thin layer of ^{X}Pu

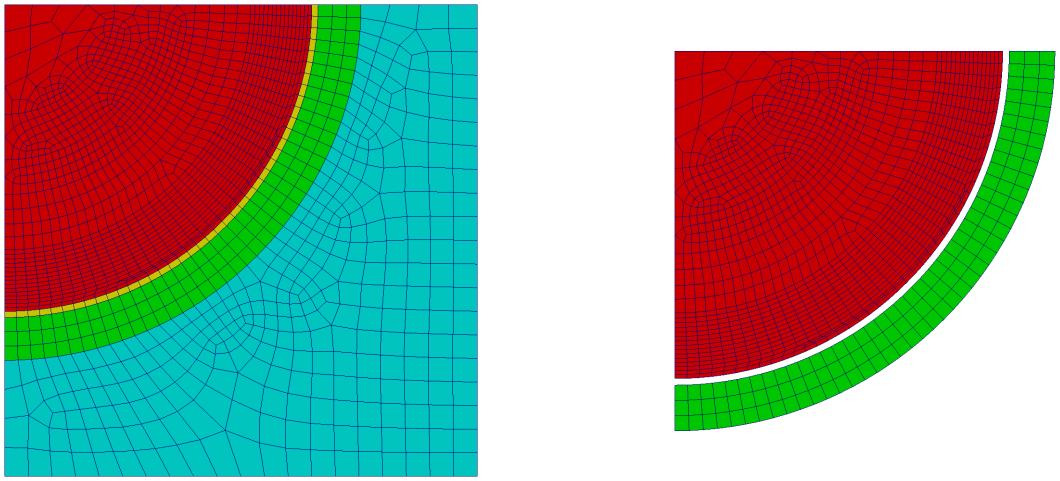

(a) RATTLES*N*AKE Mesh.

(b) BISON Mesh.

Figure 1: The fine mesh for the neutronics and fuels performance. The regions are FUEL: RED, CLADDING GREEN, GAP: YELLOW and WATER: BLUE.

builds and burns on the fuel pin's outer surface due to the absorption of epithermal neutrons. For a detailed analysis at the pin level, the absorption cross sections for the fuel pin must be spatially resolved at the fuel pin outer edge, and a high order representation or a finely resolved mesh at the rim are generally needed to better model this effect [12]. To show that RATTLES*N*AKE can simulate the rim effect, a quarter fuel pin in the (r, θ) plane was modelled neutronically. Two different meshing strategies are examined to track the buildup of the plutonium layer. An equal volume mesh has the mesh radius distribution based on dividing the total fuel pellet area into twenty equal area rings. The edge-refined mesh has five equal volumes from the pin center to 0.32766 cm (0.8 times the fuel radius) and fifteen equal volumes distributed between 0.32766 cm and 0.409575 cm to better describe where the high burnup structure developes. In the coupled calculations, the fuel, gap, cladding and water are meshed in RATTLES*N*AKE while only the fuel and cladding are meshed in BISON. The set of fuel parameters are listed in Table I, and graphics of the fine ring distributed mesh is shown in Figure 1.

3.1. PREPARATION OF THE NEUTRON CROSS SECTIONS

In order to perform a transport solution with reasonable fidelity for a pin problem, a set of cross sections that include the resonance self-shielding effects are required. The external code DRAGON4 [30] is used in this study to prepare self-shielded macroscopic cross sections, since MAMMOTH does not currently include this capability. The self-shielding calculation employs the Subgroup Projection Method (SPM) to compute moment-based probability tables instead of the traditional multi-band tables [31]. Different geometry tracking files are used for the self-shielding and flux solutions, with the latter having higher spatial resolution, as shown in Figures 2a and 2b. The geometry included in these figures shows the various azimuthally independent depletion zones as described above. Both the self-shielding and flux solutions are performed with the SHEM [32] 295 energy

Table I: The initial fuel pin parameters.

Parameter	Value
Fuel Pin Radius	4.09575 (mm)
Fuel Pin Initial Temperature	600 (K)
Outer Cladding Thickness	0.5715 (mm)
Initial Gap Thickness	0.08255 (mm)
UO_2	4.45 wt.
Cladding Initial Temperature	600 (K)
Water Temperature	585 (K)
Pitch	12.5984 (mm)
Linear Heat Rate	19.2 W/m

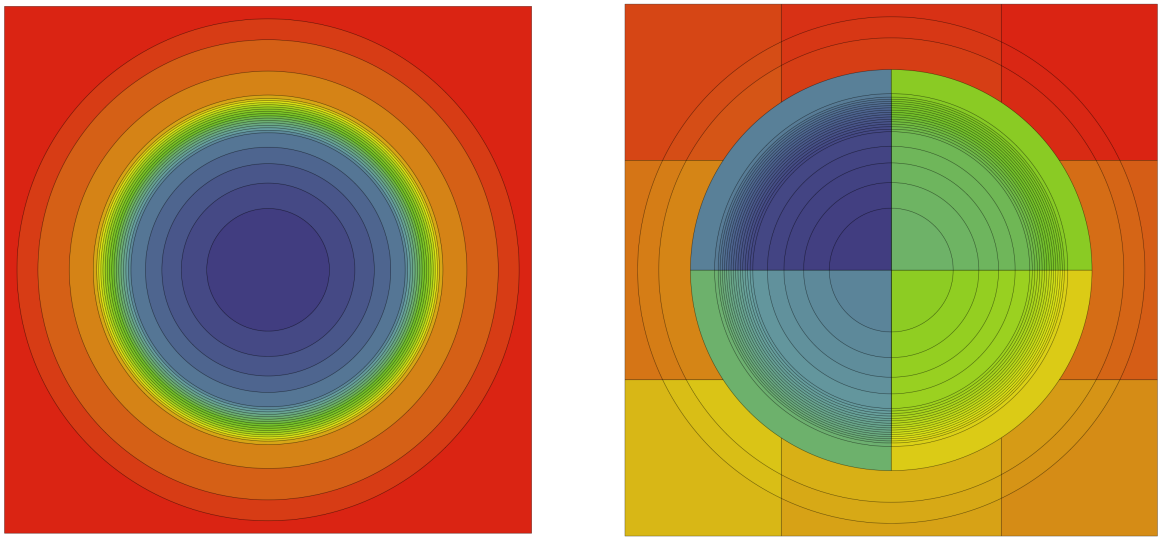

(a) Self-shielding calculation.

(b) Flux calculation.

Figure 2: DRAGON4 geometric regions used to prepare self-shielded cross sections.

group structure. The flux solution is obtained using the Method of Characteristics (MOC) with specular reflection and an angular quadrature parameter of 18 with 140 angular integration lines per centimeter. The cross sections are then spatially homogenized for each of the fifteen radial rings and condensed in energy to eight coarse energy groups. After this step, an equivalence super homogenization (SPH) technique [33] is used to prepare SPH-corrected cross sections. The pin is depleted with a 4th order Kaps-Rentrop time algorithm with the nominal state point. At each depletion step a number of fuel temperature branch cases with flat temperature distributions are computed to generate the temperature dependent cross sections. This approach is not ideal, because the flat temperature distribution tends to overestimate the resonance capture in the fuel periphery, and, consequently, tends to bias the cross sections in the outer fuel region. Nevertheless, this effect is expected to be negligible for this simulation. A tabulation is created for each ring with its local burnup and the fuel temperatures.

3.2. COUPLING UNDER MAMMOTH

Because of different mesh requirements, RATTLES*N*AKE and BISON are coupled through operator splitting. The reactor physics management application named MAMMOTH controls the execution of RATTLES*N*AKE and BISON through the MOOSE MultiApp system. MAMMOTH integrates the various MOOSE based applications and controls the depletion and core management tasks. The scalar fluxes in each energy group, the power density, and fission rate density for the various core components are calculated with RATTLES*N*AKE, and the thermomechanical effects of each fuel pin are calculated with BISON. MAMMOTH uses the power density distribution from RATTLES*N*AKE to calculate burnup on each region of the fuel pin and transmits the individual fuel pin information to the corresponding BISON application. BISON receives the information and calculates the temperature distribution and the mechanical effects of the fuel pin. In a one way coupling, the information is calculated and transmitted by MAMMOTH to the individual BISON applications. In a two way coupling, the BISON transmits the temperature distribution of each fuel pin back to MAMMOTH. The depletion step is controlled by MAMMOTH at a set of depletion points. A staggered once-through scheme is applied to the temperature cross section feed back from each fuel pin for the two way coupling. The fuel zone temperature in the fuel pin from the previous depletion step is applied to the current calculation of the cross sections.

Furthermore, there are different transfer functions inside the MOOSE MultiApp system. To avoid alteration of the power density as required in a previous coupling effort [12], the power density and the burnup values were mapped from RATTLES*N*AKE application to BISON application with element averaged values, and the neutronics and fuels performance meshes were identically meshed in their respective domains. The element mapping allows the values to be exactly reproduced from the RATTLES*N*AKE mesh to the BISON mesh. Some fidelity is lost going from a finite element nodal value to an element average value for power density and burnup, but the total power in the pellet is preserved. For the two way depletion calculation, the elemental power density and the elemental burnup values were mapped from RATTLES*N*AKE to BISON, and the nodal values temperatures were mapped from BISON back to RATTLES*N*AKE for evaluation of the cross sections in the fuel and cladding. The temperature for the water and gap are held constant by RATTLES*N*AKE in the two way calculation.

4. RESULTS

This section is subdivided into two parts. The first portion deals with the verification of the cross sections obtained from DRAGON4 to ensure that the codes produce consistent solutions. The second details the results from the coupled calculations both from the one way coupling and the two way coupling. In both sections the burnup is given in Effective Full Power Days (EFPD).

4.1. CROSS SECTION AND DEPLETION VERIFICATION

In order to verify the consistency of the macroscopic cross section libraries, a number of steady state calculations were performed at fixed temperature and fixed pin burnup. The results for the nominal case are included in Figure 3. There is good agreement between DRAGON4 and MAMMOTH. The results show a similar reactivity swing over the first 550 EFPDs of approximately 100 pcm for both non-SPH and SPH corrected cross sections. As expected, the SPH corrected cross sections pro

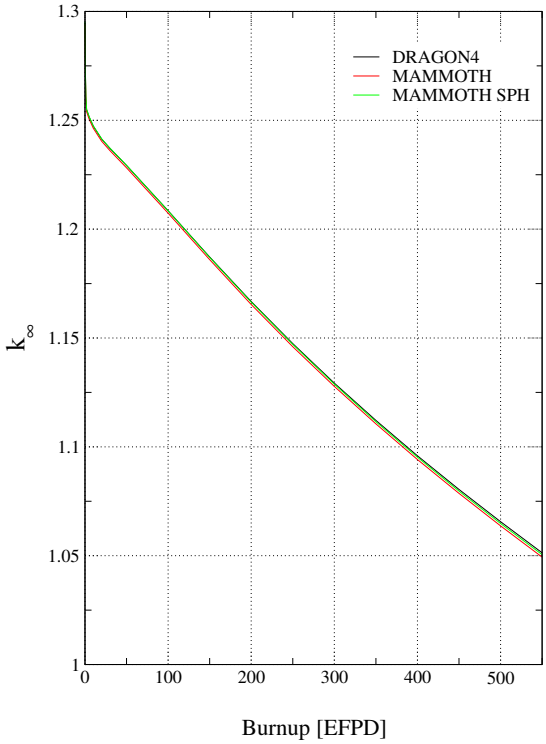

(a) Infinite multiplication factors.

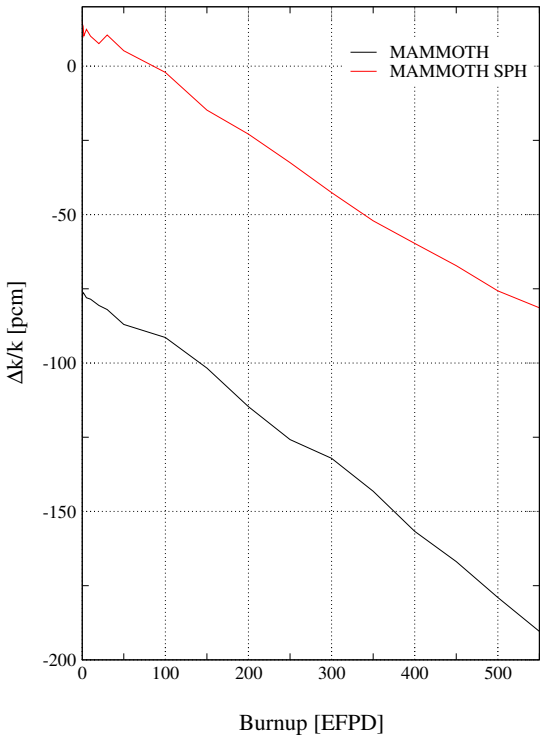

(b) Reactivity swing.

Figure 3: Verification of the cross sections obtained from a steady state calculation with and without SPH corrections at various global burnups and a nominal fuel temperature of 944.18 K.

The MAMMOTH depletion capability was verified by running a depletion to 550 EFPD tracking the local burnup in the 20 rings and using the nominal fuel temperature. The results shown in Figure 4 indicate that the capability works well and is consistent with the DRAGON4 reference solution. Note that for these runs the local ring burnup was calculated and the cross sections were interpolated with this value. Therefore, the main difference arises from variability in local burnup from both codes.

One of the purposes of this study is to replace the fixed power density distribution currently used in BISON with a power density distribution from a direct transport solution on a similar mesh. The current BISON fixed fission rate density model is based on the energy deposition from fission events and does not include all of the energy deposited in the pin by neutrons through other interactions, which might be important to resolve the high-burnup structure. DRAGON4 provides a set of energy production coefficients that are based on the mass balance of the neutron reaction, with

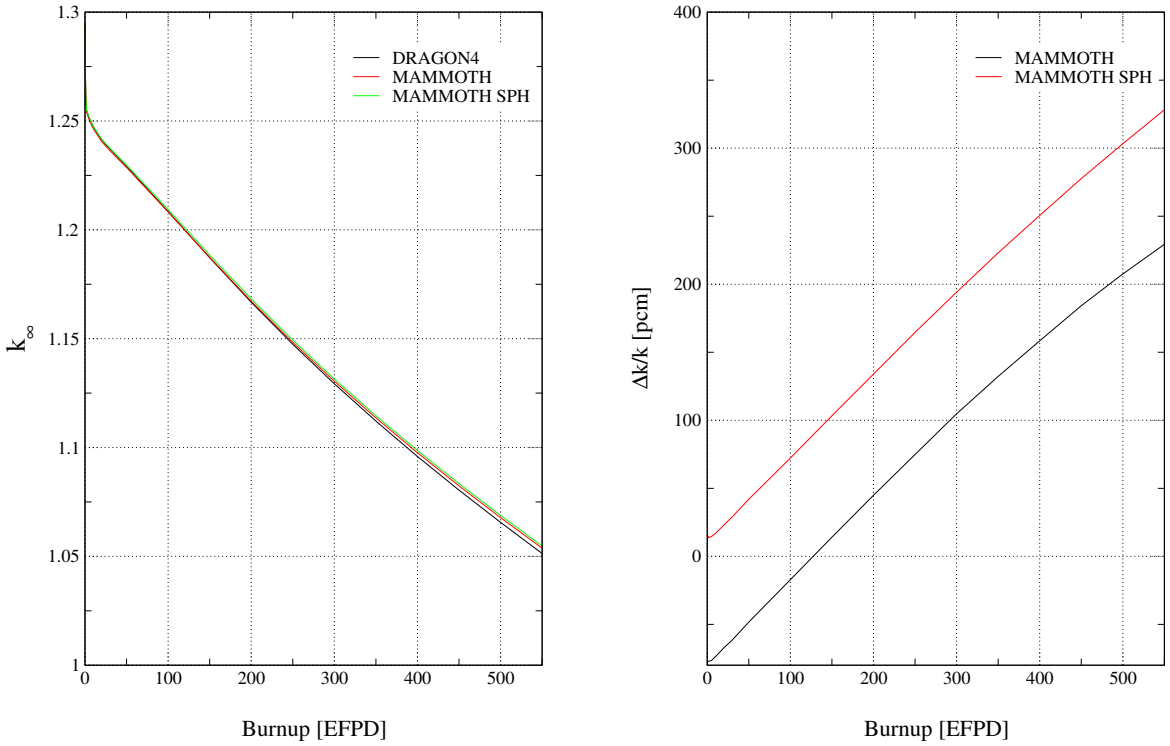

(a) Infinite multiplication factors.

(b) Reactivity swing.

Figure 4: Verification of the cross sections obtained from the depletion capability with and without SPH corrections and a nominal fuel temperature of 944.18 K.

the exception of fission. Using these energy production coefficients will, therefore, include the energy carried by gamma rays and other secondary particles. In order to verify the DRAGON4 power distribution, it was compared to a Monte Carlo reference calculation obtained with the SERPENT code [29]. Unfortunately, SERPENT does not currently have the capability to generate heating coefficients; therefore, the comparison was performed using the ^{235}U kappa values in SERPENT and the kappa values from the various isotopes in DRAGON4, shown in Figure 5. In addition, the power density distribution obtained with the DRAGON4 energy production coefficients is also included. The results show that the power density distribution based on the kappa values from DRAGON4 and SERPENT are consistent. The energy production coefficient values from DRAGON4 (shown as KERMA) yield an increase in the power density near the periphery of the pin, where the high-burnup structure develops. The neutron capture events at the periphery increase the energy deposition in this region of the pin by 2.5%, while lowering it in the region near the center of the pin. Some of this energy is due to gamma rays. This effect will need to be quantified with more detailed neutron Kinetic Energy Released in Matter (KERMA) coefficients and a coupled gamma solution.

4.2. COUPLED RESULTS

The initial pin eigenvalues and radial power distribution are calculated and compared against Monte Carlo to check the resolution of the two mesh strategies as well as the fidelity of the resolved cross sections. Table II shows the pin critical eigenvalue for the two ring meshing strategies for an in-

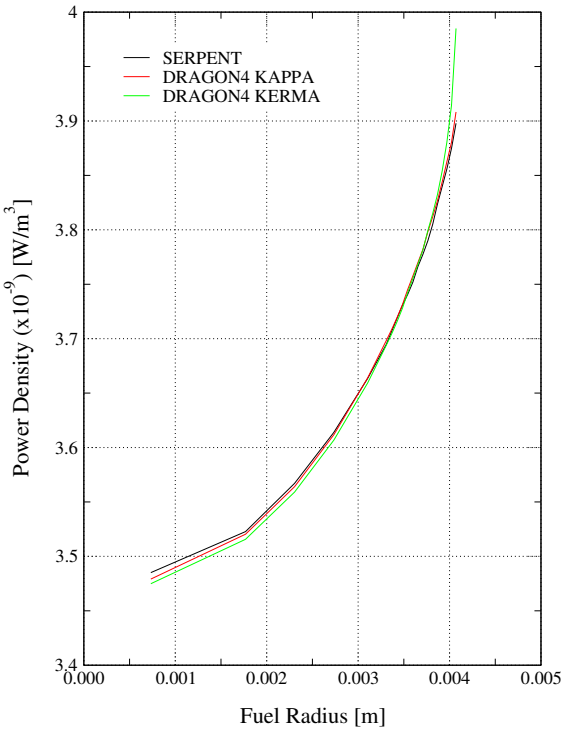

Figure 5: Comparison of DRAGON4 and SERPENT power density distributions.

Table II: RATTLES*N*AKE computed pin initial eigenvalues for fuel temperature at 1000K.

Angular Quadrature Order	Equal Volume Mesh	Edge-refined Mesh
S_2	1.29753	1.29742
S_4	1.29397	1.29386
S_8	1.29234	1.29223
S_{12}	1.29237	1.29227

creasing number of level symmetric angles. The eigenvalue calculated by SERPENT Monte Carlo for this problem is 1.29339. The eigenvalue calculated by DRAGON4 for the even ring mesh is 1.293382 and for the edge-refined mesh is 1.293294. Table II shows that both meshing strategies are a little over one hundred pcm the SERPENT Monte Carlo eigenvalue for a sufficiently resolved angular quadrature due to the group condensation and space homogenization on generating the pre-tabulated macroscopic cross sections. Figure 6 shows the initial power distribution for both meshing strategies and the converged number of level symmetric angles. In this figure the mesh with subdivided equal areas is labeled Equal and the edge boundary with the finely resolved mesh is labeled as Fine. This Fine mesh produces power distributions that are similar to those obtained with the Equal mesh, but it will result in an improved solution for the neutron capture rate and the modeling of the rim effect, since it dominates the first millimeter of fuel. As show by Table II and Figure 6, the S_8 level symmetric quadrature is sufficient to capture the inter pellet power distribution.

Figure 7 shows the reactivity curve obtained from the MAMMOTH one way calculation with a fixed fuel temperature of 600K and 1000K. For the two way MAMMOTH calculation, the feed-

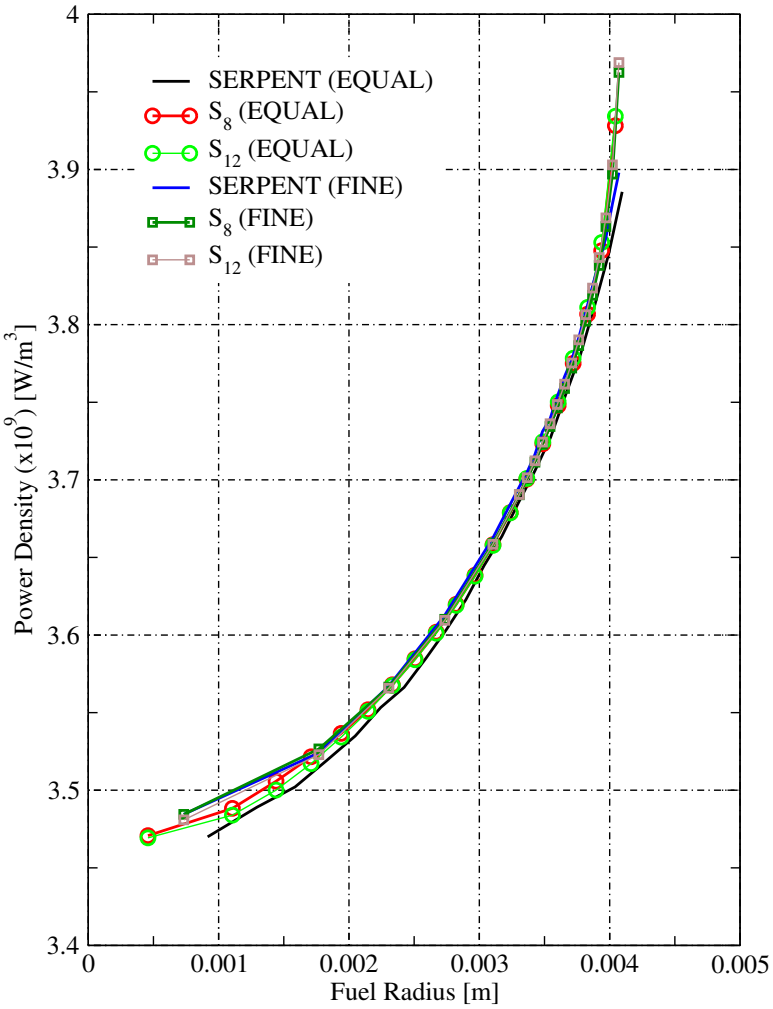

Figure 6: Initial power density distributions for SERPENT Monte Carlo and RATTLES*N*AKE with the two different meshing strategies. The S_N order is the order of the level symmetric quadrature set.

back temperature is provided by BISON. The pin is burned with the fine mesh for approximately one cycle. The code system reasonably reproduces the DRAGON4 pin eigenvalues during the depletion for the one way calculation. The eigenvalues are different for the the two way calculation and are between the 600K and 1000K eigenvalues. For the two way calculation, the average fuel temperature varies the local burnup, since the n

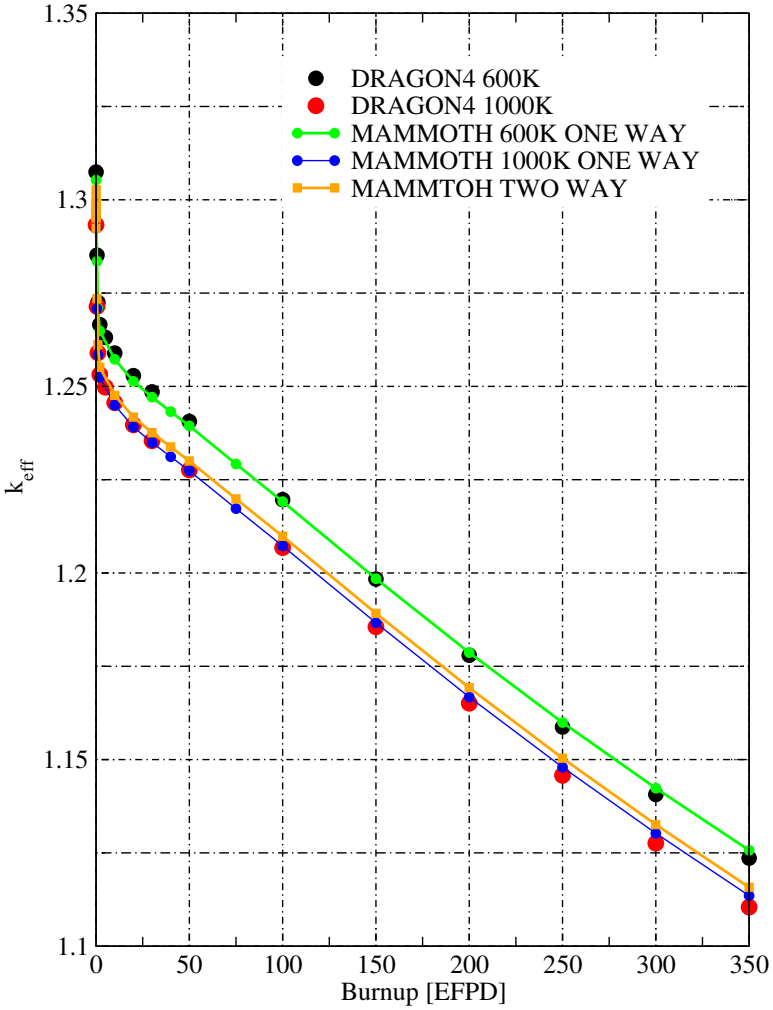

Figure 7: The pin eigenvalue as vs. Burnup. The type of coupling is listed for the MAMMOTH application, and the neutronic fuel temperature is listed for the one-way MAMMOTH and DRAGON4 results.

Results for the one way and two way coupling are shown in Figure 8, and are labled as such. As described previously, in the one way calculation only the elemental power density and the elemental burnup values are mapped from RATTLES*N*AKE to BISON. For the two way depletion calculation, the elemental power density and the elemental burnup values are mapped from RATTLES*N*AKE to BISON, and the temperatures are mapped from BISON back to RATTLES*N*AKE for evaluation of the cross sections.

In Figure 8 the power density and temperature for the fuel pellet are plotted along the diagonal at

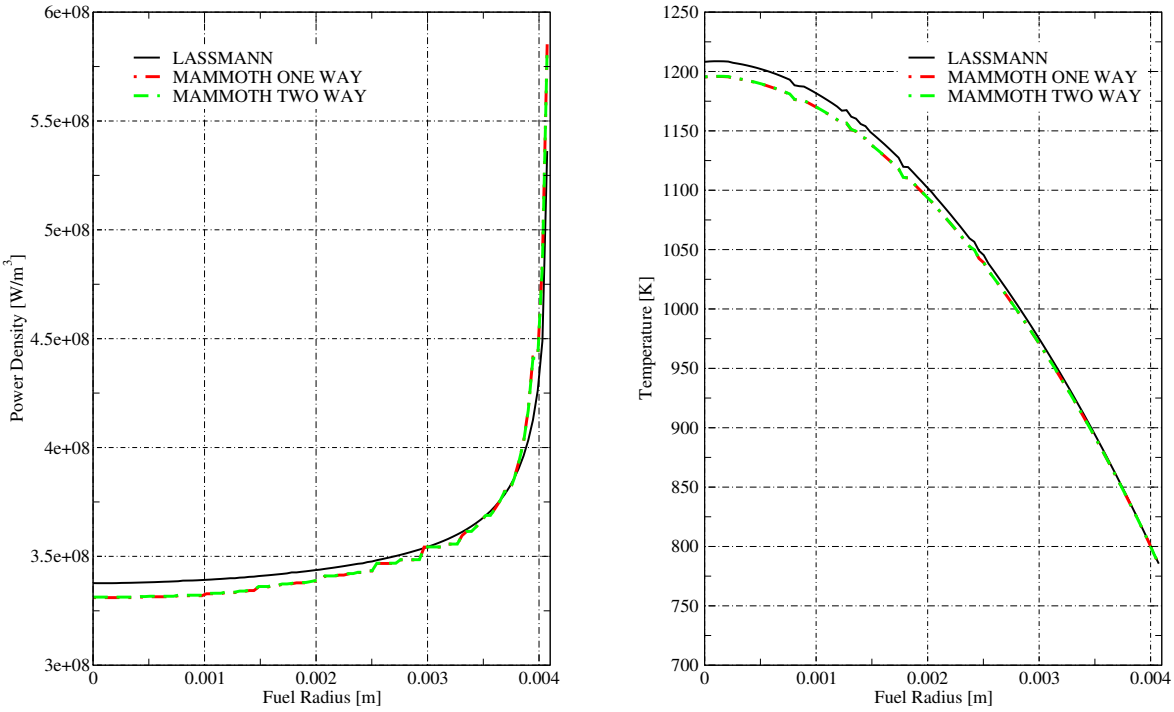

(a) Comparison of power densities

(b) Comparison of fuel temperature

Figure 8: The power density and the fuel pin temperature along the diagonal of the fuel pellet at 350 effective full power days.

350 effective full power days. The Lassmann results were obtained from a pure BISON calculation where the fission distribution was radially specified according to the radial Lassmann model distribution [6]. For these simulations, only the thermal expansion models are applied to the fuel pellet and cladding for expansion and deformation. The MAMMOTH power density distributions are slightly lower than the Lassmann density distribution towards the center of the fuel pellet and slightly higher towards the outer rim of the fuel pellet. The slight difference in power densities gives a MAMMOTH fuel pellet peak temperature that is slightly lower than the peak pellet temperature calculated with the BISON internal Lassmann style model, as would be expected. The step or shelf patterns in the MAMMOTH one way and two way results are from plotting elemental average values in the meshed rings of the fuel pellet.

In addition, the MAMMOTH one way and MAMMOTH two way calculations have the same power density, as shown in Figure 8a, but have different pin eigenvalues, as shown in Figure 7. The fission and absorption rates are similar in shape but different in magnitude for the one way and two way quasi-steady state pin eigenvalue calculations. The fission rate is scaled to produce the specified pin power, and the scaling produces power densities that are identical for this single infinite pin case.

5. CONCLUSIONS

The S_N-SAAF formulation for RATTLES*N*AKE is in agreement for the pin power density and eigenvalues when compared to SERPENT Monte Carlo and DRAGON4 calculations. For the quar-

ter infinite lattice fuel pin examined, S_8 gave sufficient agreement, and both the power density and burnup were mapped by MAMMOTH with the MultiApp system in 2-D R-θ geometry. The macro depletion also produced pin eigenvalues that were in near agreement with DRAGON4, and power density and temperature distributions that are comparable with those from the internal BISON Lassmann model.

In addition, the comparable results indicate that one way and two way coupling are feasible under the MOOSE finite element setting. Different quantities such as power density, temperature, and burnup can be communicated between the fuel resolved transport mesh and the fuels performance mesh through the MOOSE MultiApp system. Unlike previous couplings, the transfers can preserve the total rod power on LWR pin resolved meshes and can be applied to a number of different 2-D and 3-D fuel resolved calculations beyond LWR type fuels.

Furthermore, radiation transport codes with the ability to solve on unstructured meshes can produce reaction rates that are comparable to the current internal fuels performance models. Both are able to resolve the high burnup structure; however, the radiation transport code has the additional advantage taking into account local assembly element effects such as control rods and water holes and local temperature feedback effects such as fuel to cladding contact on the high burnup structure. The combined radiation transport and fuel performance package will allow greater extension as less benign conditions are modelled and the assembly elements are taken into account. Fuel performance codes can in turn inform neutronics about the effects of different fuel phenomena such as pellet clad interaction and missing pellet surface defects.

Future work includes extending this study for implicit two way coupling, as well as extending the mechanical physics to include irradiation deformation in the clad. The coupling will be applied to 2-D and 3-D problems that have fuel rods composed of discrete, smeared, and missing surface pellets, and to problems that examine the effects of assembly elements such as water holes and control rods. Future work will also include adding the capability to do micro-depletion for the fuel resolved models. These atomic densities will enable better thermal conductivity models calculated from microstructure evolution with the MOOSE application MARMOT [34] and fission gas release models in BISON.

ACKNOWLEDGEMENTS

We would like to thanks to the MOOSE team members Cody Permann, Dr. Andrew Slaughter, Dr. David Andrs, Jason Miller, and Dr. John Peterson for their support and dedication. The submitted manuscript has been authored by a contractor of the U.S. Government under Contract DE-AC07-05ID14517. Accordingly, the U.S. Government retains a non-exclusive, royalty-free license to publish or reproduce the published form of this contribution, or allow others to do so, for U.S. Government purposes.

REFERENCES

[1] H. KleyKamp. "The Chemical State of LWR High-Power Rods Under Irradiation." *Journal of Nuclear Materials*, **84**: pp. 108 – 117. URL http://dx.doi.org/doi_number (1979).

[2] Zhiwen Xu, Joel Rhodes, and Kord Smith. "CASMO-5 versus MCNP-5 Benchmark of Radial Power Profile in a Fuel Pin." In: *American Nuclear Society International Conference on Mathematics Computational Methods and Reactor Physics*. ANS. Saratoga Springs, New York, February 24 - 29 (2012).

[3] G.S. Chang and R.C. Petersen. "Validation of Radial Power Profile in FRAPCON-3 by Monte Carlo Method." In: *Transactions of the American Nuclear Society*, volume 85, (pp. 385 – 386). ANS. Reno, Nevada, November 11 - 15 (2001).

[4] Chan Bock Lee *et al.* "RAPID model to predict radial burnup distribution in LWR UO2 fuel." *Journal of Nuclear Materials*, **282(1)**: pp. 196 – 204 (2000).

[5] P Botazzoli *et al.* "Applying Advanced Neutron Transport Calculations for Improving Fuel Performance Codes." In: *Proceedings of Top Fuel*. ANS. Paris, France, September 6 - 10 (2009).

[6] K. Lassmann, C.T. Walker, and J. van de Laar. "Extension of the transuranus burnup model to heavy water reactor conditions." *Journal of Nuclear Materials*, **255**: pp. 222 – 233 (1998).

[7] Mathieu Hursin, Thomas J Downar, and Justin Thomas. "PWR Control Rod Ejection Analysis with the Method Characteristic Code DeCART." In: *PHYSOR 2008 International Conference on the Physics of Reactors Nuclear Power: A Sustainable Resource*. ANS. Interlaken, Switzerland, September 14 - 19 (2008).

[8] Gerardo Grandi *et al.* "Effect of CASMO-5 Cross Section Data and Doppler Temperature Definitions on LWR Reactivity Initiated Accidents." In: *PHYSOR 2010 Advance in Reactor Physics to Power the Nuclear Renaissance*. ANS. Pittsburg, Pennsylvania USA, May 9 - 14 (2010).

[9] Han Gyu Joo *et al.* "Consistent Comparison of Monte Carlo and Whole-Core Transport Solutions for Cores with Thermal Feedback." In: *PHYSOR 2004 The Physics of Fuel Cycles and Advanced Nuclear Systems: Global Developments*. ANS. Chicago, Illionios USA, April 25 - 29 (2004).

[10] Sergei Lemehov, Jinichi Nakamura, and Montoe Suzuki. "Pluton: a Three Group Model for the Radial Distribution of Plutonium, Burnup, and Power Profiles in Highly Irradiated LWR Fuel Rods." *Nuclear Technology*, **133**: pp. 153 – 168 (2001).

[11] Mathieu Hursin, Thomas J Downar, and Robert Montgomery. "Impact of Improved Neutronic Methodology on the Cladding Response during a PWR reactivity initiated accident." *Nuclear Engineering and Design*, **262**: pp. 180 – 188 (2013).

[12] Frederick N. Gleicher *et al.* "Coupling the Core Analysis Program DeCART to the Fuel Performance Application BISON." In: *International Conference on Mathematics and Computational Methods Applied to Nuclear Science and Engineering*. ANS. Sun Valley, Idaho, May 5 - 9 (2013).

[13] Steve Hamilton *et al.* "Integrated Radiation Transport and Nuclear Fuel Performance for Assembly-Level Simulations." In: *PHYSOR 2012 Advances in Reactor Physics Linking Research Industry adn Education*. ANS. Knoxvill, Tenessee USA, April 15 - 20 (2012).

[14] Motoe Suzuki *et al. Light Water Reactor Fuel Analysis Code FEMAXI-7; Model and Structure*. *Technical Report 2013-005*, Japan Atomic Energy Agency (2013).

[15] Han Gyu Joo *et al.* "Method and Performance of a Three-Dimensiona Whole-Core Transport Code DeCART." In: *PHYSOR 2004 The Physics of Fuel Cycles and Advanced Nuclear Systems: Global Developments*. ANS. Chicago, Illinois, April 25 - 29 (2004).

[16] Richard L Williamson *et al.* "Multidimensional multiphysics simulation of nuclear fuel behavior." *Journal of Nuclear Materials*, **423**: pp. 149 – 163 (2012).

[17] Tomas Downar *et al. PARCS U.S. NRC Core Simulator v.2.6 Theory Manual*. U.S. NRC, Rockville, Maryland USA (2004).

[18] W.F. Lyon *et al.* "Capabilities of the FALCON steady state and transient fuel performance code." In: *Proceedings of the 2004 International Meeting on LWR Fuel Performance*. ANS. Orlando, Florida USA, September 19 - 22 (2004).

[19] Thomas M Evans *et al.* "Devno: A new Three-Dimensional Parallel Discrete Ordinates Code in Scale." *Nuclear Technology*, **2010(2)**: pp. 171–200. URL http://dx.doi.org/doi_number (2010).

[20] Steve Hamilton and Kevin Clarno. "Mathematical Framework for the Coupling of AMP and Denovo Codes." In: *Transactions of the American Nuclear Society*, volume 105, (pp. 515–517). ANS (2011).

[21] Derek Gaston *et al.* "MOOSE: A parallel computational framework for coupled systems of nonlinear equations." *Nuclear Engineering and Design*, **239**: pp. 1768 – 1778 (2009).

[22] Dana A Knoll and DE Kyes. "Jacobian-free newton-krylov methods a survey of approaches and applications." *Journal of Computational Physics*, **193**: pp. 357 – 397 (2004).

[23] J. E. Morel and J. M. McGhee. "A self-adjoint angular flux equation." *Nucl. Sci. Eng.*, **132**: pp. 312–325 (1999).

[24] J. E. Morel *et al.* "Spatial discretizations for self-adjoint forms of the radiative transfer equations." *Journal of Computational Physics*, **214**: pp. 12–40 (2006).

[25] J. Liscum-Powell. *Finite Element Numerical Solution of a Self-Adjoint Transport Equation for Coupled Electron-Photon Problems*. *Technical Report SAND2000-2017*, Sandia National Laboratory (2000).

[26] J. L. Liscum-Powell *et al.* "Finite element solution of the self-adjoint angular flux equation for coupled electron-photon transport." *Nucl. Sci. Eng.*, **142**: pp. 270–291 (2002).

[27] Y. Wang. "Nonlinear diffusion acceleration for the multigroup transport equation discretized with s_n and continuous FEM with Rattle$s_n$ake." In: *Proceedings of the International Conference on Mathematics and Computational Methods Applied to Nuclear Science & Engineering*

(M&C 2013). http://www.inl.gov/technicalpublications/Documents/5723137.pdf (2013).

[28] E. E. Lewis and W. F. Miller. *Computational Methods of Neutron Transport*. John Wiley & Sons (1984).

[29] J. Lepp anan. *Development of a new Monte Carlo Reactor Physics Code*. Ph.D. thesis, Helsinki University of Technology (2007).

[30] G. Marleau, A. Hébert, and R. Roy. *A user guide for dragon version4*. Ecole Polytechnique de Montr'eal, Montr'eal, Canida (2013).

[31] A. Hébert. "Development of the subgroup projection method for resonance self-shielding calculations." *Nucl. Sci. Eng.*, **162**: pp. 56 – 75 (2009).

[32] A. Hébert and A. Santamarina. "Refinement of the santamarina-hfaiedh energy mesh between 22.5 ev and 11.4 kev." In: *International Conference on the Physics of Reactors,PHYSOR'08*. Interlaken, Switzerland September 14 - 19 (2008).

[33] A. Hébert and G. Mathonniere. "Development of a third-generation superhomogenization method for the homogenization of a pressurized water reactor assembly." *Nuc. Sci. Eng.*, **115**: pp. 129–141 (1993).

[34] Michael R. Tonks *et al.* "An object-oriented finite elmenet framework for multiphysics phase field simulations." *Computational Material Science*, **51(3)**: p. 2012 (2012).